Analysis of Fiber-Reinforced Elastomeric Isolators

James M. Kelly

Professor in the Graduate School, Earthquake Engineering Research Center, University of California, Berkeley, USA

ABSTRACT: *An analysis is given for the mechanical characteristics of multilayer elastomeric isolation bearings where the reinforcing elements-normally steel plates-are replaced by a fiber reinforcement. The fiber-reinforced isolator, in contrast to the steel-reinforced isolator (which is assumed to be rigid both in extension and flexure), is assumed to be flexible in extension, but completely without flexural rigidity. The influence of fiber flexibility on the mechanical properties of the fiber-reinforced isolator, such as vertical and horizontal stiffness, is studied, and it is shown that it should be possible to produce a fiber-reinforced isolator that matches the behavior of steel-reinforced isolator. The fiber-reinforced isolator will be significantly lighter and could lead to a much less labor intensive manufacturing process.*

Keywords: Base isolator; Fiber-reinforced; Isolator; Seismic isolation; Light-weight isolator; Low-cost isolator

1. INTRODUCTION

Seismic isolation technology in the United States today is applied almost entirely to large, expensive buildings housing sensitive internal equipment, for example, computer centers, chip fabrication factories, emergency operation centers, and hospitals. The isolators used in these applications are large, expensive, and heavy. An individual isolator can weigh one ton and often more. To extend this valuable earthquake-resistant strategy to housing and commercial buildings, it is necessary to reduce the cost and weight of the isolators.

The primary weight in an isolator is due to the reinforcing steel plates, which are used to provide the vertical stiffness of the rubber-steel composite element. A typical rubber isolator has two large end-plates (around 1 inch thick) and 20 thin reinforcing plates (1/8 inches thick). The high cost of producing the isolators results from the labor involved in preparing the steel plates and laying-up of the rubber sheets and steel plates for vulcanization bonding in a mold. The steel plates are cut, sand-blasted, acid cleaned, and then coated with bonding compound. Next, the compounded rubber sheets with the interleaved steel plates are put into a mold and heated under pressure for several hours to complete the manufacturing process. The purpose of this research is to suggest that both the weight and the cost of isolators can be reduced by eliminating the steel reinforcing plates and replacing them with a fiber reinforcement.

The weight reduction is possible as fiber materials are available with an elastic stiffness that is of the same order as steel. Thus the reinforcement needed to provide the vertical stiffness may be obtained by using a similar volume of very much lighter material. The cost savings may be possible if the use of fiber allows a simpler, less labor-intensive manufacturing process. It is also possible that the current approach of vulcanization under pressure in a mold with steam heating can be replaced by microwave heating in an autoclave.

Another benefit to using fiber reinforcement is that it would then be possible to build isolators in long rectangular strips, whereby individual isolators could be cut to the required size. All isolators are currently manufactured as either circular or square in the mistaken belief that if the isolation system for a building is to be isotropic, it needs to be made of symmetrically shaped isolators. Rectangular isolators in the form of long strips would have distinct advantages over square or circular isolators when applied to buildings where the lateral resisting system is constituted of walls. When isolation is applied to buildings with structural walls, additional wall beams are needed to carry the wall from isolator to isolator. A strip isolator would have a distinct advantage for retrofitting masonry structures and for isolating residential housing constructed from concrete or masonry blocks.

In modeling the isolator reinforced with steel plates, the plates are assumed to be inextensional and rigid in flexure. The fiber reinforcement is made up of many individual fibers grouped in strands and coiled into a cord of submillimeter diameter. The cords are more flexible in tension than the individual fibers therefore they may stretch when the bearing is loaded by the weight of a building. On the other hand, they are completely flexible in bending, so the assumption made when modeling current

isolators-that plane sections remain plane-no longer holds. In fact, when a fiber-reinforced isolator is loaded in shear, a plane cross section becomes curved. This leads to an unexpected advantage in the use of fiber reinforcement. When the bearing is displaced in shear, the tension in the fiber bundle (which acts on the curvature of the reinforcing sheet caused by the shear) produces a frictional damping that is due to individual strands in the fiber bundle slipping against each other. This energy dissipation in the reinforcement adds to that of the elastomer. Recent tests show that this energy dissipation is larger than that of the elastomer. Therefore, when designing a fiber-reinforced isolator for which a specified level of damping is required, it is not necessary to use elaborate compounding to provide the damping, but to use the additional damping from the fiber.

To calculate the vertical stiffness of a steel-reinforced bearing, an approximate analysis is used that assumes that each individual pad in the bearing deforms in such a way that horizontal planes remain horizontal and points on a vertical line lie on a parabola after loading. The plates are assumed to constrain the displacement at the top and bottom of the pad. Linear elastic behavior with incompressibility is assumed, with the additional assumption that the normal stress components are approximated by the pressure. This leads to the well-known "pressure solution", which is generally accepted as an adequate approximate approach for calculating the vertical stiffness. The extensional flexibility of the fiber reinforcement can be incorporated into this approach, and that predictions of the resulting vertical stiffness can be made.

The horizontal stiffness and buckling of the steel-reinforced isolator is modeled by an equivalent beam theory whereby a bearing with many discrete pads is replaced by a continuous composite beam with plane sections normal to the undeformed axis assumed to remain plane but not normal to the deformed axis, reflecting the very low shear stiffness of the rubber and the flexural rigidity of the steel reinforcement. When the reinforcement is perfectly flexible in bending, the beam model must be extended to permit the warping of the cross section. As a preliminary step in constructing the appropriate model for the isolator, a beam theory is developed here for a linear elastic beam that parallels the familiar strength-of-materials approach to beam theory, but includes a new displacement variable, which measures the warping of the section and uses a warping shape function that uncouples the warping of the section from the axial deformation and the rotation. For the rectangular cross section, this function is a Legendre polynomial.

Linear elastic behavior is assumed. A stress field is derived from the strains in terms of the displacement variables and stress resultants are defined. These include the usual axial forces, bending moment and shear, plus two additional resultants associated with warping. These resultants are related back to the kinematic variables by a set of sectional elastic constants. Since we have no intuitive feeling for the equilibrium of these additional resultants, the sectional equations of equilibrium are obtained by formal integration of the equations of stress equilibrium across the section.

For a typical beam, the warping of the cross section has very little influence on the mechanical behavior of the beam, but it can have a large influence on an isolator, which is essentially a short beam with very low shear stiffness. If flexible reinforcement is used, it might reduce the horizontal stiffness and the buckling load. The modeling of the isolator by beam theory is complicated by the fact that the normal stresses in the rubber are given by the so-called pressure solution. For example, the axial stress across the section is parabolic and the bending stress cubic, so that selecting a warping shape function that uncouples the warping resultants from the axial load and the bending moment needs to take the pressure solution into account. Such a warping shape function is found, and the resultant theory follows that for the beam. Predictions of the effect of the flexibility of the reinforcement on the horizontal stiffness of the isolator are made.

The theoretical analyses of vertical and horizontal stiffnesses and the buckling of the fiber-reinforced isolator have been supplemented by experimental work, and while the tests are only preliminary, they indicate that the concept is viable. The vertical stiffness of the model isolators is in the range of stiffnesses of practical designs of steel-reinforced bearings, with the same diameter (12 inches) and the same thickness of rubber (4 inches). The hysteresis loops generated under combined compression and shear have effective stiffnesses that are somewhat (~20%) less than those are the equivalent steel-reinforced bearing, but have the same general characteristics and show stable behavior up to a peak shear strain of 150% (the limit of the testing machine).

Much recent discussion has focused on "smart" rubber bearings and "intelligent" base isolation systems as the new thrust in seismic isolation research. While there may be a role for these adaptive systems for large expensive buildings in highly seismic areas, the development of light-weight, low-cost isolators is crucial if this method of seismic protection is to be applied to a wide range of buildings, such as housing, schools, and medical centers, in earthquake-prone areas of the world.

2. VERTICAL STIFFNESS OF FIBER-REINFORCED BEARINGS

The essential characteristic of the elastomeric isolator is the very large ratio of the vertical stiffness relative to the horizontal stiffness. This is produced by the reinforcing plates, which in current industry standard are thin steel plates. These plates prevent lateral bulging of the rubber, but allow the rubber to shear freely. The vertical stiffness

can be several hundred times the horizontal stiffness. The steel reinforcement has a similar effect on the resistance of the isolator to bending moments, usually referred to as the "tilting stiffness". This important design quantity makes the isolator stable against large vertical loads.

2.1. Compression of Pad with Rigid Reinforcement

Before developing the solution for the flexible reinforcement, it is useful to review the theory for the rigid reinforcement. A linear elastic theory is the most common method used to predict the compression and the tilting stiffness of a thin elastomeric pad. The first analysis of the compression stiffness was done using an energy approach by Rocard [1]; further developments were made by Gent and Lindley [2] and Gent and Meinecke [3]. The theory given here is a simplified version of these analyses and is applicable to bearings with shape factors greater than around five.

The analysis is an approximate one based on a number of assumptions. The kinematic assumptions are as follows:

(i) points on a vertical line before deformation lie on a parabola after loading

(ii) horizontal planes remain horizontal

We consider an arbitrarily shaped pad of thickness t and locate a rectangular Cartesian coordinate system, (x, y, z), in the middle surface of the pad, as shown in Figures 1a and 1b shows the displacements, (u, v, w) in the coordinate directions under assumptions (i) and (ii):

$$u(x,y,z) = u_0(x,y)\left(1-\frac{4z^2}{t^2}\right)$$

$$v(x,y,z) = v_0(x,y)\left(1-\frac{4z^2}{t^2}\right) \qquad (1)$$

$$w(x,y,z) = w(z)$$

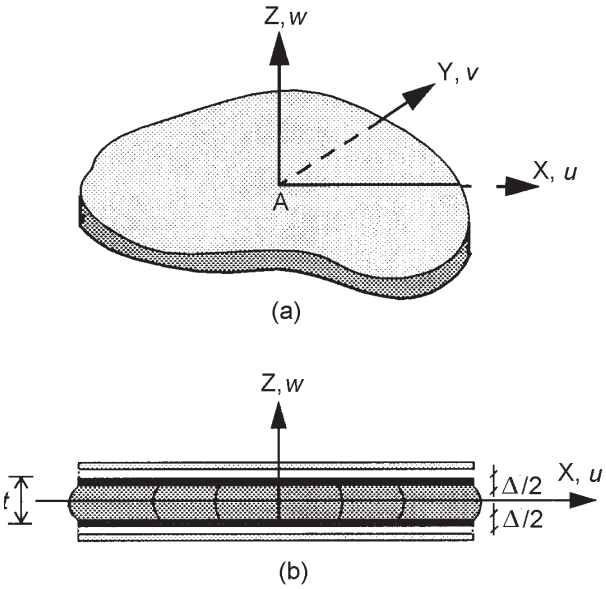

Figure 1. Constrained rubber pad and coordinate system.

This displacement field satisfies the constraint that the top and bottom surfaces of the pad are bonded to rigid substrates. The assumption of incompressibility produces a further constraint on the three components of strain, in the form of

$$\varepsilon_{xx} + \varepsilon_{yy} + \varepsilon_{zz} = 0 \qquad (2)$$

and this leads to:

$$(u_{0,x} + v_{0,y})\left(1-\frac{4z^2}{t^2}\right) + w_{,z} = 0$$

where the commas imply partial differentiation with respect to the indicated coordinate. When integrated through the thickness this gives

$$u_{0,x} + v_{0,y} = \frac{3\Delta}{2t} \qquad (3)$$

where the change of thickness of the pad is Δ ($\Delta > 0$ in compression).

The stress state is assumed to be dominated by the internal pressure, p, such that the normal stress components, τ_{xx}, τ_{yy}, τ_{zz}, differ from $-p$ only by terms of order $(t^2/l^2)p$, i.e.,

$$\tau_{xx} \approx \tau_{yy} \approx \tau_{zz} \approx -p\left[1 + O\left(\frac{t^2}{l^2}\right)\right]$$

where l is a typical dimension of the pad. The shear stress components, τ_{xz} and τ_{yz}, which are generated by the constraints at the top and bottom of the pad, are assumed to be of order $(t/l)p$; the in-plane shear stress, τ_{xy}, is assumed to be of order $(t^2/l^2)p$.

The equations of equilibrium for the stresses

$$\begin{aligned} &\tau_{xx,x} + \tau_{xy,y} + \tau_{xz,z} = 0 \\ &\tau_{xy,x} + \tau_{yy,y} + \tau_{yz,z} = 0 \\ &\tau_{xz,x} + \tau_{yz,y} + \tau_{zz,z} = 0 \end{aligned}$$

reduce under these assumptions to:

$$\begin{aligned} &\tau_{xx,x} + \tau_{xz,z} = 0 \\ &\tau_{yy,y} + \tau_{yz,z} = 0 \end{aligned} \qquad (4)$$

Assuming that the material is linearly elastic, then shear stresses τ_{xz} and τ_{yz} are related to the shear strains, γ_{xz} and γ_{yz}, by

$$\tau_{xz} = G\gamma_{xz} \quad , \quad \tau_{yz} = G\gamma_{yz}$$

with G being the shear modulus of the material; thus,

$$\tau_{xz} = -8Gu_0\frac{z}{t^2} \quad , \quad \tau_{yz} = -8Gv_0\frac{z}{t^2} \qquad (5)$$

From the equilibrium equations, therefore,

$$\tau_{xx,x} = \frac{-8Gu_0}{t^2} \quad , \quad \tau_{yy,y} = \frac{-8Gv_0}{t^2} \qquad (6)$$

which when inverted to give u_0, v_0 and inserted into the incompressibility condition gives

$$\frac{t^2}{8G}(\tau_{xx,xx}+\tau_{yy,yy})=\frac{3\Delta}{2t} \tag{7}$$

In turn, by identifying both τ_{xx} and τ_{yy} as $-p$, this reduces to:

$$p_{,xx}+p_{,yy}=\nabla^2 p=-\frac{12G\Delta}{t^3}=-\frac{12G}{t^2}\varepsilon_c \tag{8}$$

where $\varepsilon_c=\Delta/t$ is the compression strain. The boundary condition, $p=0$, on the perimeter, C, of the pad completes the system for $p(x, y)$.

The vertical stiffness of a rubber bearing is given by the formula

$$K_V=\frac{E_c A}{t_r}$$

where A is the area of the bearing, t_r is the total thickness of rubber in the bearing, and E_c is the instantaneous compression modulus of the rubber-steel composite under the specified level of vertical load. The value of E_c for a single rubber layer is controlled by the shape factor, S, defined as

$$S=\frac{loaded\ area}{free\ area}$$

which is a dimensionless measure of the aspect ratio of the single layer of the elastomer. For example, in an infinite strip of width $2b$, and with a single layer thickness of t, $S=b/t$, and for a circular pad of diameter ϕ, and thickness t,

$$S=\phi/(4t)$$

and for a square pad of side a and thickness t,

$$S=a/(4t)$$

To determine the compression modulus, E_c, we solve for p and integrate over A to determine the resultant load, P; E_c is then given by

$$E_c=\frac{P}{A\varepsilon_c} \tag{9}$$

where A is the area of the pad.

For example, for an infinite strip of width $2b$ (see Figure 2), Eq. (8) reduces to:

$$\nabla^2 p=\frac{d^2 p}{dx^2}=-\frac{12G}{t^2}\varepsilon_c$$

which, with $p=0$ at $x=\pm b$, gives

$$p=\frac{6G}{t^2}(b^2-x^2)\varepsilon_c$$

In this case the load per unit length of the strip, P, is given by

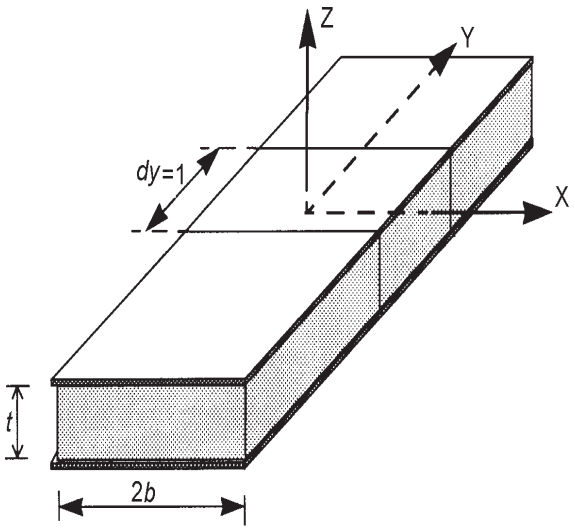

Figure 2. Infinitely long rectangular pad showing dimensions.

$$P=\int_{-b}^{b} p\,dx=\frac{8Gb^3}{t^2}\varepsilon_c$$

Since the shape factor, $S=b/t$, and the area per unit length is $A=2b$,

$$E_c=\frac{P}{A\varepsilon_c}=4GS^2 \tag{10}$$

2.2. Compression Stiffness with Flexible Reinforcement

Developing the solution for the compression of a pad with rigid reinforcement is algebraically simple enough to be treated in two dimensions and for an arbitrary shape. The problem for the pad with flexible reinforcement is more complicated, however; for simplicity, the derivation will be developed for a long, rectangular strip. As before, the rubber is assumed incompressible and the pressure is assumed to be the dominant stress component. The kinematic assumption of quadratically variable displacement is supplemented by an additional displacement that is constant through the thickness and is intended to accommodate the stretching of the reinforcement. Thus

$$u(x,z)=u_0(x)\left(1-\frac{4z^2}{t^2}\right)+u_1(x) \tag{11}$$

$$w(x,z)=w(z)$$

The constraint of incompressibility means

$$\varepsilon_{xx}+\varepsilon_{zz}=0$$

leading to:

$$u_{0,x}\left(1-\frac{4z^2}{t^2}\right)+u_{1,x}+w_{,z}=0$$

Integration through the thickness with respect to z leads to:

$$u_{0,x}+\frac{3}{2}u_{1,x}=\frac{3\Delta}{2t} \tag{12}$$

The only equation of stress equilibrium in this case is $\tau_{xx,x}+\tau_{xz,z}=0$, and the assumption of elastic behavior means that

$$\tau_{xz}=G\gamma_{xz} \tag{13}$$

which with

$$\gamma_{xz}=-\frac{8z}{t^2}u_0 \tag{14}$$

from Eq. (11), gives

$$\tau_{xx,x}=\frac{8Gu_0}{t^2}$$

The individual fibers are replaced by an equivalent sheet of reinforcement of thickness t_f. The internal force, $F(x)$, per unit width of the equivalent reinforcing sheet is related to the shear stresses on the top and bottom of the pad by

$$\frac{dF}{dx}-\tau_{xz}\Big|_{z=\frac{t}{2}}+\tau_{xz}\Big|_{z=-\frac{t}{2}}=0$$

as shown in Figure 3.

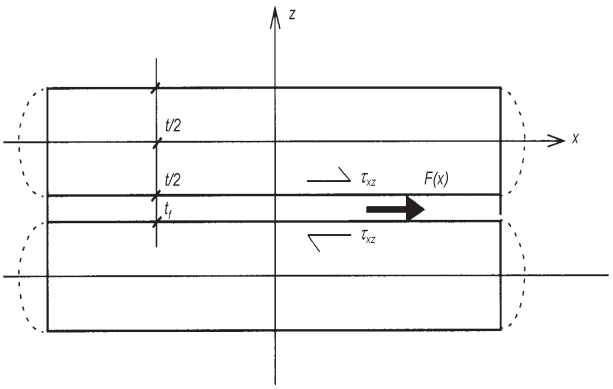

Figure 3. Force in equivalent sheet of reinforcement.

From Eqs. (13) and (14) we have

$$\tau_{xz}\Big|_{z=\frac{t}{2}}=-\frac{8Gu_0}{2t};\tau_{xz}\Big|_{z=-\frac{t}{2}}=\frac{8Gu_0}{2t}$$

giving

$$\frac{dF}{dx}=-\frac{8Gu_0}{t} \tag{15}$$

The extensional strain in the reinforcement ε_f is related to the stretching force through the elastic modulus of the reinforcement E_f and the thickness t_f such that

$$\varepsilon_f=u_{1,x}=\frac{F}{E_f t_f} \tag{16}$$

which when combined with Eq. (15), gives

$$u_{1,xx}=-\frac{8G}{E_f t_f t}u_0$$

The complete system of equations is

$$\tau_{xx,x}=-\frac{8Gu_0}{t^2} \tag{17}$$

$$u_{0,x}+\frac{3}{2}u_{1,x}=\frac{3\Delta}{2t} \tag{18}$$

$$u_{1,xx}=\frac{8G}{E_f t_f t}u_0 \tag{19}$$

with boundary conditions or symmetric conditions as follows:

$$u_0(0)=0$$

$$u_1(0)=0$$

$$\tau_{xx}(\pm b)=0$$

$$F(\pm b)=0$$

Furthermore, the assumption that

$$\tau_{xx}=\tau_{zz}=-p$$

gives

$$\int_{-b}^{b}\tau_{xx}dx=-p$$

where p is the resultant load per unit length on the bearing.

Combining Eqs. (18) and (19) to eliminate u_0, gives

$$u_{1,xxx}-\frac{12G}{E_f t_f t}u_{1,x}=-\frac{12G}{E_f t_f t}\cdot\frac{\Delta}{t} \tag{20}$$

Assuming $\alpha^2=12G/E_f t_f t$, u_1 becomes:

$$u_1=A+B\cosh\alpha x+C\sinh\alpha x+\frac{\Delta}{t}x$$

Symmetry suggests that $A=0, B=0$, giving

$$u_1=C\sinh\alpha x+\frac{\Delta}{t}x$$

From Eq. (16) we have

$$F=E_f t_f u_{1,x}=E_f t_f\left(\alpha C\cosh\alpha x+\frac{\Delta}{t}\right)$$

which with $F=0$ on $x=\pm b$ leads to:

$$F(x)=\frac{\Delta}{t}E_f t_f\left(1-\frac{\cosh\alpha x}{\cosh\alpha b}\right)$$

$$u_1(x)=\frac{\Delta}{t}\left(x-\frac{\sinh\alpha x}{\alpha\cosh\alpha b}\right)$$

$$u_0(x) = \frac{3}{2}\frac{\Delta}{t}\frac{sinh\,\alpha x}{\alpha\, cosh\,\alpha b}$$

Also, using Eq. (17) and the boundary condition $\tau_{xx} = 0$ at $x = \pm b$ gives

$$\tau_{xx} = -\frac{\Delta}{t}\frac{E_f t_f}{t}\left(1 - \frac{cosh\,\alpha x}{cosh\,\alpha b}\right)$$

The pressure assumption gives

$$P = \frac{E_f t_f}{t} 2\int_0^b \left(1 - \frac{cosh\,\alpha x}{cosh\,\alpha b}\right) dx \frac{\Delta}{t}$$

$$= \frac{2E_f t_f}{\alpha t}(\alpha b - tanh\,\alpha b)\frac{\Delta}{t}$$

which can be interpreted as an effective compression modulus, E_c given by

$$E_c = \frac{P}{\Delta}\frac{\Delta}{t} = \frac{E_f t_f}{t}\left(1 - \frac{tanh\,\alpha b}{\alpha b}\right) \qquad (21)$$

Two extreme cases can be used to verify the accuracy of these results. When $\alpha \to 0$, i.e. $E_f \to \infty$, and $tanhx = x - \frac{x^3}{3} + \frac{2x^5}{15}$, E_c becomes:

$$E_c = \frac{E_f t_f}{t}\left(1 - \frac{\alpha b - \frac{\alpha^3 b^3}{3} - \frac{2\alpha^5 b^5}{15}}{\alpha b}\right)$$

$$= \frac{E_f t_f}{t}\frac{\alpha^2 b^2}{3}\left(1 - \frac{2}{5}\alpha^2 b^2\right)$$

$$= 4G\frac{b^2}{t^2}\left(1 - \frac{2}{5}\alpha^2 b^2\right)$$

Thus with $\alpha \to 0$, $E_c = 4GS^2$ as before. The formula also shows that $E_c < 4GS^2$ for all finite values of E_f.

On the other hand, if $\alpha \to \infty$, then $E_c = E_f \frac{t_f}{t}$. This is harder to interpret, but it comes from the fact that $\alpha \to \infty$ is equivalent to $G \to \infty$, i.e., the deformation is uniform, as shown in Figure 4. Coupled with incompressibility, we have

$$\varepsilon_f = \frac{\Delta}{t}$$

The work done by load P is $\frac{1}{2}P\Delta$ and the strain energy of the reinforcement is $\frac{1}{2}E_f\varepsilon_f^2\, 2bt_f$. Equating the two gives

$$P = (E_f\, 2bt_f / t^2)\Delta$$

or

$$E_c = \frac{E_f t_f}{t}$$

The effect of the elasticity of the reinforcement on the various quantities of interest can be illustrated by a few examples. Normalizing the compression modulus, E_c, from

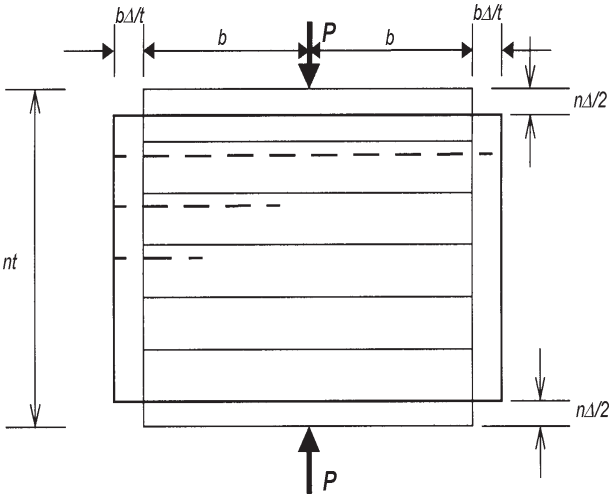

Figure 4. Extreme case $\alpha b \to \infty\ (G \to \infty)$.

Eq. (21) by $4GS^2$, results to:

$$\frac{E_c}{4GS^2} = \frac{3}{\alpha^2 b^2}\left(\frac{1 - tanh\,\alpha b}{\alpha b}\right)$$

which is shown in Figure 5 for $0 \le \alpha b \le 5$. Note how the stiffness decreases with decreasing E_f. The distribution of the pressure for various values αb from $\alpha b = 0$, corresponding to $E_f = \infty$ (the steel pressure solution), to $\alpha b = 3$, corresponding to very flexible reinforcement is shown in Figure 6. The displacement pattern for the reinforcement and for the force in the reinforcement for these values of ab are shown in Figures 7 and 8. As the reinforcement becomes more flexible, the displacement tends to almost linear in x and the force is almost constant.

An alternative way to look at the effect of the reinforcement is to note that the important parameter is the normalized reinforcement stiffness

$$\lambda = \frac{E_f t_f t}{Gb^2} = \frac{12}{\alpha^2 b^2}$$

The pattern of the overall compression modulus, E_c, in terms of reinforcement modulus is shown in Figure 9.

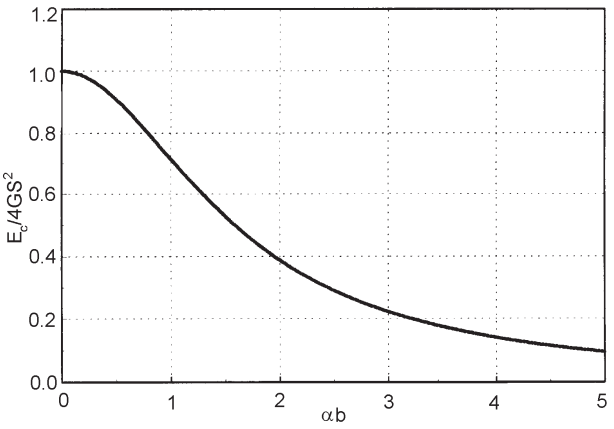

Figure 5. Normalized effective compression modulus as a function of $\alpha b = (12Gb^2 / E_f t_f t)^{1/2}$.

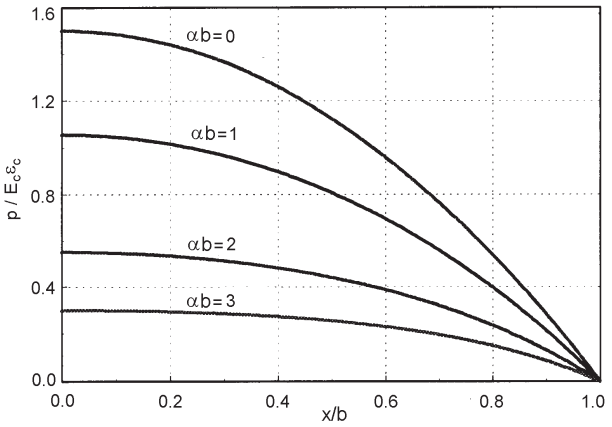

Figure 6. Pressure distributions for various values of αb .

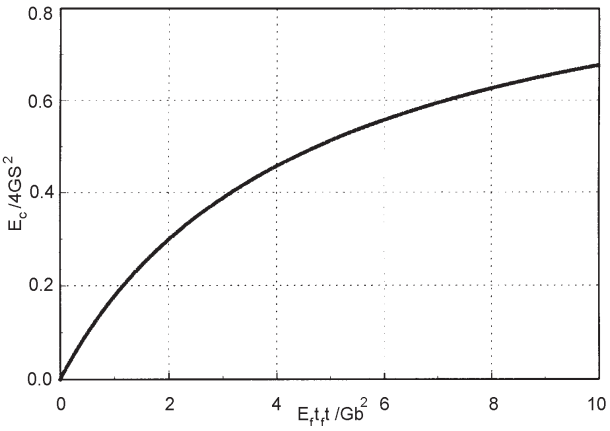

Figure 9. Normalized compression modulus as a function of normalized reinforcement modulus.

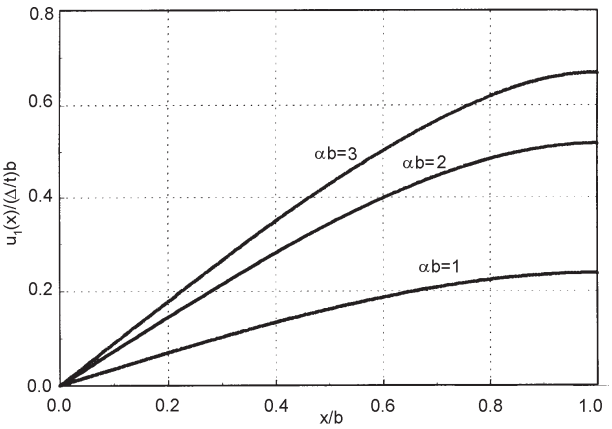

Figure 7. Displacement pattern for fiber reinforcement for various values of αb .

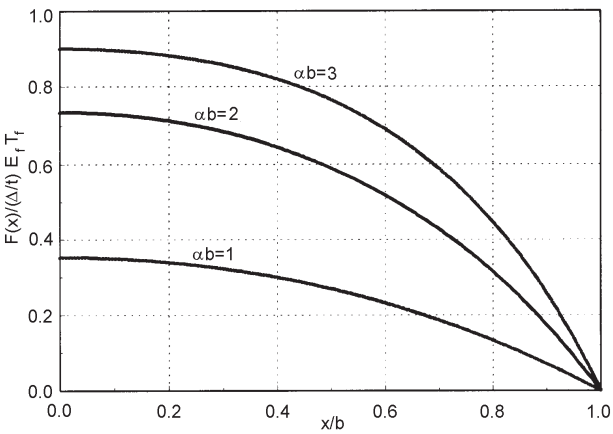

Figure 8. Normalized force pattern in reinforcement.

Several samples of fiber-reinforced bearings were constructed to verify the viability of the approach. These bearings were 12 inches in diameter, either 4 inches or 6 inches thick, and reinforced by twisted strands of Kevlar have been tested in compression. The elastic modulus of this reinforcement corresponded to a value of λ of around 50, representing very stiff reinforcement. The force-displacement curves for the four tests are shown in Figure 10.

The bearings were handmade. The top and bottom surfaces were not very flat, and the reinforcement was not taut before loading, which caused significant run-in before the bearings began to develop vertical stiffness. The vertical stiffnesses show a certain amount of scatter, reflecting the amateurish method of construction, but the average effective modulus, E_c, was 49 ksi, which with a steel-reinforced bearing and a rubber modulus of 100 psi, would mean a shape factor of 9. Clearly, these bearings prove that it is relatively easy to match the stiffness of a typical steel bearing with fiber reinforcement.

2.3. Tilting Stiffness with Rigid Reinforcement

The tilting stiffness is computed using a similar argument as before. The displaced configuration, however, is obtained in two stages. First the deformation, shown dotted in Figure 11, which is what would occur if the bending conformed to elementary beam theory is visualized. Since this cannot satisfy the incompressibility constraint, a further pure shear deformation is superimposed. The displacement field is given by

$$u(x,y,z) = u_0(x,y)\left(1-\frac{4z^2}{t^2}\right)-\theta\frac{z^2}{2t}$$

$$v(x,y,z) = v_0(x,y)\left(1-\frac{4z^2}{t^2}\right) \qquad (22)$$

$$w(x,y,z) = \frac{\theta z x}{t}$$

Here, θ is the angle between the rigid plates in the deformed configuration and the bending is about the y-axis. The radius of curvature, ρ, generated by the deformation is related to θ by

$$\frac{1}{\rho} = \frac{\theta}{t}$$

The incompressibility condition Eq. (2) when integrated through the thickness becomes:

$$u_{0,x} + v_{0,y} + \frac{3}{2}\frac{\theta}{t}x = 0$$

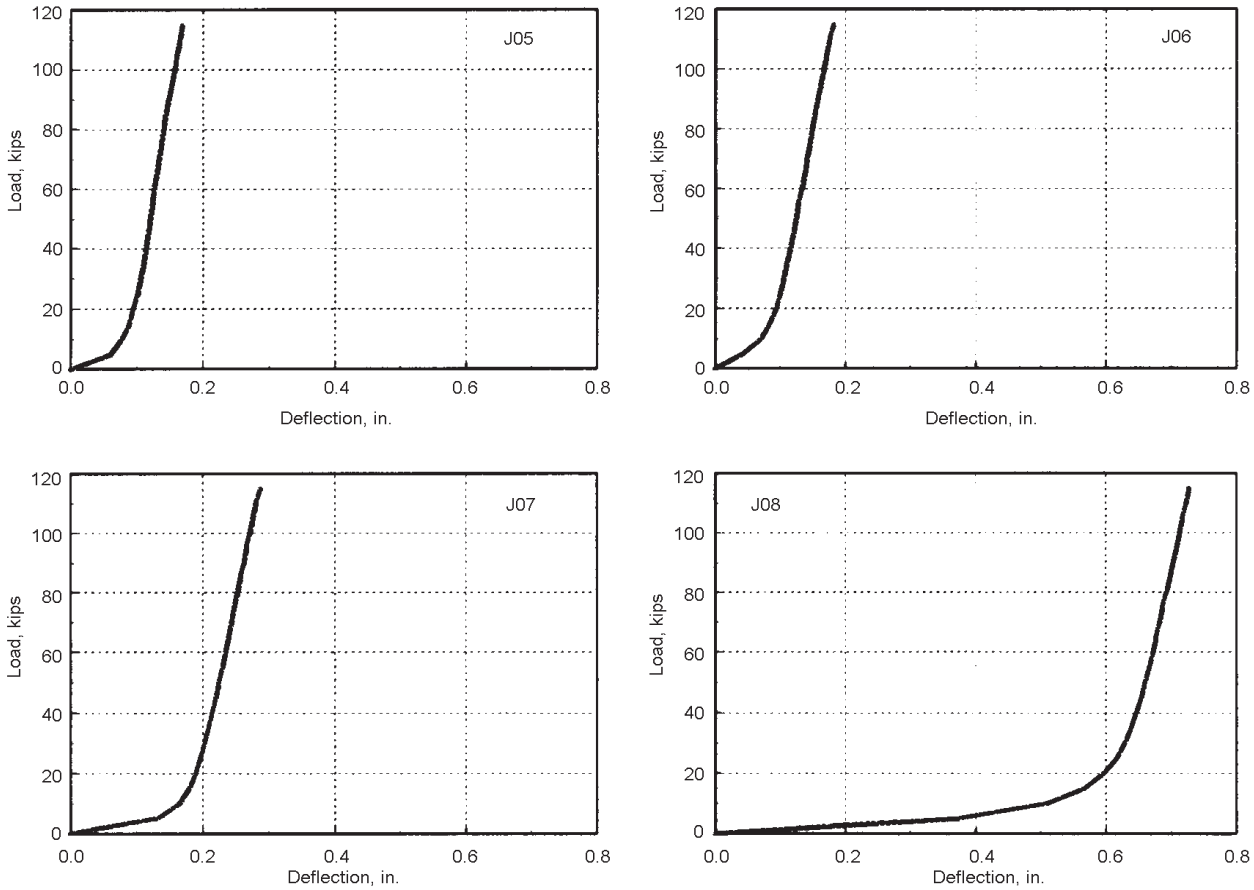

Figure 10. Force-displacement diagrams for 12in. diameter bearings in compression.

The shear stresses, τ_{xz}, τ_{yz}, are given by

$$\tau_{xz} = -\frac{8Gz}{t^2} u_0 \quad , \quad \tau_{yz} = -\frac{8Gz}{t^2} v_0$$

and substitution into the equations of equilibrium gives

$$u_0 = -\frac{t^2}{8G} p_{,x} \quad , \quad v_0 = -\frac{t^2}{8G} p_{,y}$$

which with the incompressibility condition leads to:

$$\nabla^2 p = p_{,xx} + p_{,yy} = \frac{12\theta G}{t^3} x \tag{23}$$

with $p = 0$ on the edges.

For the definite strip width of $2b$, shown in Figure 11, we have

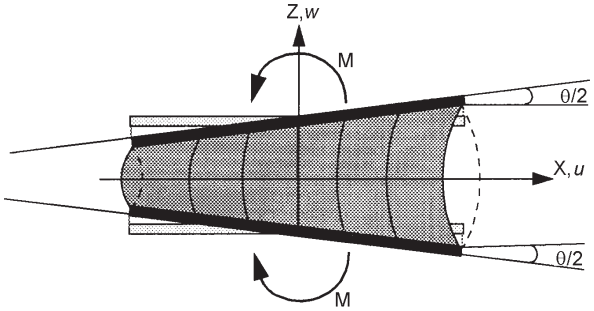

Figure 11. Pad in pure flexure.

$$p_{,xx} = \frac{12\theta G x}{t^3}$$

or

$$p = \frac{12\theta G}{t^3}(x^2 - b^2)x \tag{24}$$

The resultant moment, M, is given by

$$M = -\int_{-b}^{b} px\,dx = \frac{8\theta G b^5}{15t^3} \tag{25}$$

Comparing Eq. (25) with the usual bending equation for a beam, namely, $M = EI/\rho$, where I is the moment of inertia of a beam cross section with the shape of the pad, and identify E by $E_c = 4GS^2$, where $S = b/t$, and $EI = 2E_c b^3/15$. Thus the effective I for the strip becomes equal to $2b^3/15$. This reduction is due to the pressure distribution varying cubically across the width of the strip, whereas in a beam, the stress distribution is linear.

2.4. Tilting Stiffness with Flexible Reinforcement

The derivation of the tilting stiffness starts with the addition of the stretching term $u_1(x)$ to the displacement assumption of Eq. (22), giving

$$u(x, z) = u_0(x)\left(1 - \frac{4z^2}{t^2}\right) + u_1(x) - \theta\frac{z^2}{2t}$$

$$w(x,z)=\frac{\theta z x}{t} \tag{26}$$

As before, the curvature $1/\rho=\theta/t$.

Incompressibility and integration across the thickness leads to:

$$u_{0,x}+\frac{3}{2}u_{1,x}=\frac{3\theta x}{2t}$$

Combining the shear stress-strain relation with the equation of stress equilibrium gives $\tau_{xx,x}=\frac{8G}{t^2}u_0$, and, as before, the force in the reinforcement is given by

$$\frac{dF}{dx}=-\frac{8Gu_0}{t}$$

leading to:

$$u_{1,xx}=-\frac{8G}{E_f t_f t}u_0$$

The complete system of equations is

$$\tau_{xx,x}=\frac{8Gu_0}{t^2};\quad \tau_{xx}(\pm b)=0 \tag{27}$$

$$u_{0,x}+\frac{3}{2}u_{1,x}=\frac{3\theta}{2t}x \tag{28}$$

$$u_{1,xx}=-\frac{8G}{E_f t_f t}u_0 \tag{29}$$

$$F(x)=E_f t_f u_{1,x};\qquad F(\pm b)=0 \tag{30}$$

By eliminating u_0, it becomes:

$$u_{1,xxx}-\frac{12G}{E_f t_f t}u_{1,x}=\frac{12G}{E_f t_f t}\frac{\theta x}{t} \tag{31}$$

As before the resulting solutions with $\alpha^2=12G/E_f t_f t$ are

$$u_1=\frac{\theta b}{t}\left(\frac{\cosh\alpha x}{\alpha\sinh\alpha b}-\frac{x^2}{\alpha b}\right) \tag{32}$$

$$u_0=-\frac{E_f t_f t}{8G}\alpha\frac{\theta b}{t}\left(\frac{\cosh\alpha x}{\alpha\sinh\alpha b}-\frac{1}{\alpha b}\right) \tag{33}$$

$$F(x)=E_f t_f t\frac{\theta b}{t}\left(\frac{\sinh\alpha x}{\sinh\alpha b}-\frac{x}{b}\right) \tag{34}$$

$$\tau_{xx}(x)=-E_f t_f\frac{\theta b}{t}\left(\frac{\sinh\alpha x}{\sinh\alpha b}-\frac{x}{b}\right) \tag{35}$$

The effective bending stiffness is calculated from

$$M=\int_{-b}^{b}\tau_{xx}\,x\,dx=\frac{E_f^2 t_f^2}{6Gt}\theta b\left(1+\frac{\alpha^2 b^2}{3}-\frac{\alpha b}{\tanh\alpha b}\right)$$

giving

$$(EI)_{eff}=\frac{M}{\theta/t}=\frac{E_f^2 t_f^2 b}{6G}\left(1+\frac{\alpha^2 b^2}{3}-\frac{\alpha b}{\tanh\alpha b}\right) \tag{36}$$

When $E_f\to\infty$, $\alpha\to 0$, and using $coth x=\frac{1}{x}+\frac{x}{3}-\frac{x^3}{45}+\ldots$ Eq. (36) becomes:

$$(EI)_{eff}\to\frac{E_f^2 t_f^2 b}{6G}\left(1+\frac{\alpha^2 b^2}{3}-1-\frac{\alpha^2 b^2}{3}+\frac{\alpha^4 b^4}{45}+\ldots\right)$$

$$=\frac{E_f^2 t_f^2 b}{6G}\left(\frac{12G}{E_f t_f t}\right)^2\frac{b^4}{45}$$

$$=\frac{24Gb^5}{45t^2}=\frac{1}{5}4GS^2\frac{2}{3}b^3$$

$$=\frac{1}{5}(E_c)I$$

2.5. Extension to Variable Deflection Pattern

The basic pressure solution with rigid reinforcement is correct to within the kinematic and stress assumptions made in the derivation. The two strain functions in the case of the rigid reinforcement that form the right hand sides of Eqs. (8) and (23), namely $\Delta/t=\varepsilon_c$ and $(\theta/t)x$ are adequate for predicting the response of an isolator to horizontal shear and for analyzing the stability of the isolator. When the reinforcement is perfectly flexible in bending, it is necessary to extend Eqs. (8) and (23) to a variable deflection pattern *w(x, y)*.

Because the individual pads are thin compared with their width and the variation in the displacement in the lateral direction is small, it will be assumed that the displacement Δ and θx can be replaced by *w*, so that the pressure solution in this case is given by

$$\nabla^2 p=\frac{12G}{I^3}w(x,y)$$

3. SHEARING DEFORMATION OF ISOLATORS WITH REINFORCEMENT WITH NO FLEXURAL RIGIDITY

3.1. Beam Theory with Warping Deformation Included

In this section the modeling of an isolator with fiber reinforcement that is undergoing lateral (shear) deformation will be discussed. It is assumed that the vertical load has been applied to the isolator and the reinforcement is in tension. It is also assumed that shear deformation will produce no change in the tension in the reinforcement, but that the reinforcement is perfectly flexible in bending.

The isolator is modeled as a continuous composite beam made up of many pads of elastomeric material. To differentiate the beam theory analysis from the previous

analysis, we use a different coordinate system and different notation. Coordinate x_1 will denote distance along the beam, and x_2 and x_3 the principal directions of the beam cross-section; indicial notation σ_{ij} and ε_{ij} will be used for the stresses and strains in the beam.

Before developing a theory for the isolator with flexible reinforcing plates, it is useful to develop the theory for a simple beam of rectangular cross section and to obtain the response of this beam model to simple shear. The theory could be extended to arbitrary cross sections, albeit with a considerable increase in algebraic complexity, but for the purpose of illustration the rectangular section is adequate. The geometry of the beam is shown in Figure 12.

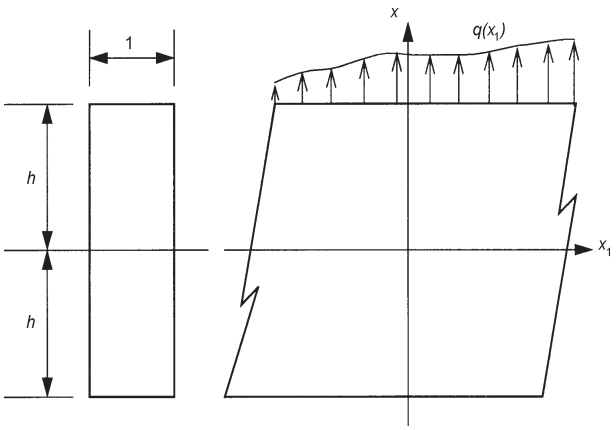

Figure 12. Beam model showing dimensions and shear loading.

The deformation of the beam is characterized by four displacement variables, u, v, ψ and ϕ, all of which are functions of x_1. The displacement field, (u_1, u_2), shown in Figure 13, is taken to be

$$u_1 = u(x_1) - \psi(x_1)x_2 + \phi(x_1)f_w(x_2)$$
$$u_2 = v(x_1) \tag{37}$$

The function ψ is the average angle of rotation of the section and ϕ is the measure of the warping of the section. The functions u and v are the displacement of the middle surface in the x_1 and x_2 directions. It is convenient to select the function $f_w(x_2)$ to be orthogonal to both 1 and x_2 so that no rotation of the section is produced by $f_w(x_2)$; thus the product ϕf_w can be identified as the deviation from a planar displacement field, or in other words, the warping of the section.

The appropriate form of $f_w(x_2)$ for the rectangular section is

$$f_w(x_2) = \left(\frac{x_2}{h}\right)^3 - \frac{3}{5}\left(\frac{x_2}{h}\right) \tag{38}$$

The selection of $f_w(x_2)$ to be dimensionless means the warping function, $\phi(x_1)$, has units of displacement. The resulting strains are

$$\varepsilon_{11} = u' - \psi' x_2 + \phi' f_w$$

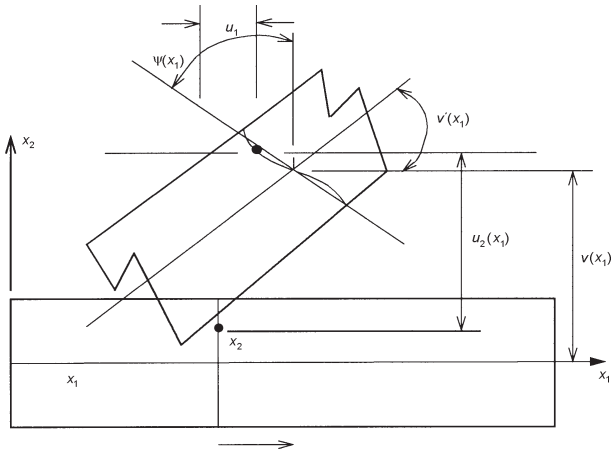

Figure 13. Displacement of field of beam with shear and warping.

$$2\varepsilon_{12} = (\upsilon' - \psi) + \phi f_w' \tag{39}$$

and assuming elastic behavior the stresses become:

$$\sigma_{11} = Eu' - E\psi' x_2 + E\phi' f_w(x_2)$$
$$\sigma_{12} = G(\upsilon' - \psi) + G\phi f_w'(x_2) \tag{40}$$

Defining a set of stress resultants by

$$N = \int_A \sigma_{11} dA$$
$$M = -\int_A \sigma_{11} x_2 dA$$
$$Q = \int_A f_w(x_2)\sigma_{11} dA \tag{41}$$
$$V = \int_A \sigma_{12} dA$$
$$R = \int_A f_w'(x_2)\sigma_{12} dA$$

The resultants are related to the kinematic variables by

$$N = EAu'$$
$$M = EI\psi' \tag{42}$$
$$Q = EJ\phi'$$

and

$$V = GA(\upsilon' - \psi) + GB\phi$$
$$R = GB(\upsilon' - \psi) + GC\phi \tag{43}$$

where

$$A = \int_A dA = 2h$$
$$I = \int_A x_2^2 dA = \frac{2}{3}h^3$$
$$J = \int_A f_w^2(x_2) dA = \frac{8}{175}h \tag{44}$$
$$B = \int_A f_w'(x_2) dA = \frac{4}{5}$$

$$C = \int_A [f_w'(x_2)]^2 dA = \frac{48}{25h}$$

Substitution back into the stress equations gives

$$\sigma_{11} = \frac{N}{A} - \frac{M}{I} x_2 + \frac{Q}{J} f_w(x_2)$$

$$\sigma_{12} = \frac{CV - BR}{AC - B^2} - \frac{BV - AR}{AC - B^2} f_w'(x_2) \tag{45}$$

The equilibrium equations for the stress resultants are derived from the equilibrium equations for the stress, namely

$$\sigma_{11,1} + \sigma_{12,2} = 0$$

$$\sigma_{12,1} + \sigma_{22,2} = 0 \tag{46}$$

Integrating the first through the thickness and assuming zero external shear on $x_2 = \pm h$

$$N' = 0 \tag{47}$$

Multiplying the first by x_2 and integrating gives

$$M' + V = 0 \tag{48}$$

and multiplying the first by $f_w(x_2)$ and integrating through the thickness gives

$$Q' - R = 0 \tag{49}$$

Finally, integrating the second equation of equilibrium through the thickness gives

$$V' + q = 0 \tag{50}$$

where $q(x)$ is the external load per unit length on the beam.

When the resultants are replaced by the kinematic variables, we have

$$EI\psi'' + GA(\upsilon' - \psi) + GB\phi = 0 \tag{51}$$

$$GA(\upsilon' - \psi') + GB\phi' = -q \tag{52}$$

$$EJ\phi'' - GB(\upsilon' - \psi) - GC\phi = 0 \tag{53}$$

The problem to which we intend to apply these equations is that of a beam under end shears, V, with constraints against rotation and warping at each end, as shown in Figure 14. The problem is clearly anti-symmetric in displacement υ and symmetric in ψ and ϕ. The shear force is constant throughout the beam and the moment is

$$M = -Vx \tag{54}$$

The equations for the displacement variables, υ, ψ and ϕ, reduce to:

$$EI\psi' = -Vx \tag{55}$$

$$GA(\upsilon' - \psi) + GB\phi = V \tag{56}$$

$$EJ\phi'' - GB(\upsilon' - \psi) - GC\phi = 0 \tag{57}$$

From Eq. (56) we have

$$\upsilon' - \psi = -\frac{B}{A}\phi + \frac{V}{GA} \tag{58}$$

and this inserted into Eq. (57) gives

$$EJGA\,\phi'' - [GAGC - (GB)^2]\phi = GBV \tag{59}$$

The alternative form in terms of $(\upsilon' - \psi)$ is

$$EJGA(\upsilon' - \psi)'' + [GAGC - (GB)^2](\upsilon' - \psi) = -GCV \tag{60}$$

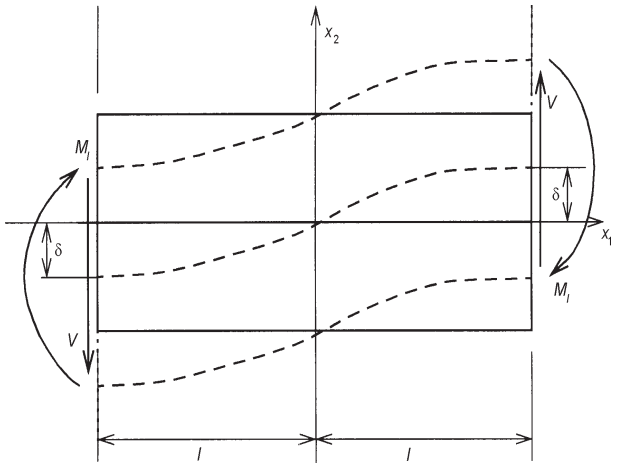

Figure 14. Beam model under shear end load.

The solutions for these are

$$\phi = C_1 \cosh\omega x_1 - \frac{GB}{GAGC - (GB)^2} V$$

and

$$\upsilon' - \psi = D_1 \cosh\omega x_1 - \frac{GC}{GAGC - (GB)^2} V$$

where

$$\omega^2 = \frac{GAGC - (GB)^2}{EJGA}$$

and where C_1 and C_2 are related through Eq. (58) as

$$D_1 \cosh\omega x_1 + \frac{C}{AC - B^2}\frac{V}{G} = -\frac{B}{A}\cdot\left(C_1 \cosh\omega x_1 - \frac{B}{AC - B^2}\frac{V}{G}\right) + \frac{V}{GA}$$

i.e.,

$$D_1 = -\frac{B}{A} C_1$$

The boundary conditions at $x_1 = \pm l$ require that both ψ and ϕ vanish and this determines that

$$\phi(x_1) = -\frac{B}{AC - B^2}\left(1 - \frac{\cosh\omega x_1}{\cosh\omega l}\right)\frac{V}{G} \tag{61}$$

and

$$\upsilon' - \psi = \frac{V}{GA}\left(\frac{AC}{AC-B^2} - \frac{B^2}{AC-B^2}\frac{cosh\omega x_1}{cosh\omega l}\right) \tag{62}$$

From Eq. (55) we have

$$\psi = -\frac{V}{EI}\frac{x_1^2}{2} + C_3$$

and since $\psi(\pm l) = 0$,

$$\psi = \frac{V}{2EI}(l^2 - x_1^2) \tag{63}$$

To complete the solution we substitute for ψ in Eq. (62) and integrate giving

$$\upsilon(x_1) = \frac{V}{2EI}\left(l_1^2 x_1 - \frac{x_1^3}{3}\right)$$

$$-\left(\frac{B^2}{AC-B^2}\frac{1}{\omega}\frac{sinh\omega x_1}{cosh\omega l} - \frac{AC}{AC-B^2}x_1\right)\frac{V}{GA}$$

where we have set $\upsilon(0)$ to maintain the anti-symmetry of the solution for $\upsilon(x_1)$. The deflections at each end are $\pm\delta$ where

$$\delta = \frac{Vl^3}{3EL} + \frac{Vl}{GA}\left(\frac{AC}{AC-B^2} - \frac{B^2}{AC-B^2}\frac{tanh\,\omega l}{\omega l}\right)$$

For the rectangular section considered here

$$\frac{AC}{AC-B^2} = \frac{6}{5}$$

and

$$\frac{B^2}{AC-B^2} = \frac{1}{5}$$

so that if we suppress the warping by setting $EJ \to \infty$, i.e., ϕ everywhere zero, then $\omega l \to 0$, and δ_s, the part of δ due to shear, becomes:

$$\delta_s \to \frac{Vl}{GA}$$

On the other hand, to model the case where there is no restraint on the warping at the end of the beam, the warping stiffness EJ is set to zero, then

$$\lambda l \to \infty$$

and

$$\delta_s \to \frac{6Vl}{5GA} = \frac{Vl}{G}\frac{1}{\frac{5A}{6}}$$

which corresponds to the usual theory of shear deformation in beams. Furthermore, if ϕ is not constrained and either $EJ \to 0$ or alternatively $\phi'' \to 0$, then

$$\phi = -\frac{B}{C}(\upsilon' - \psi)$$

and

$$\sigma_{12} = G\left[1 - \frac{B}{C}f_{w'}(x_2)\right](\upsilon' - \psi)$$

which with Eq. (46) gives

$$\sigma_{12} = \frac{3V}{2A}\left(1 - \frac{x_2^2}{h^2}\right)$$

Thus, if the effect of the warping is not included, the solution reduces to the standard beam theory with shear deformation included. The influence of the constraint of the warping depends on the parameter ωl, which is given by

$$(\omega l)^2 = \frac{G}{E}\frac{AC-B^2}{JA}l^2 = \frac{35G}{E}\frac{l^2}{h^2}$$

It follows that ω is likely to be large and the solution for $\phi(x_1)$ near $x = \pm l$ can be written as

$$\phi(x_1) = -\frac{AB}{AC-B^2}[1 - e^{-\omega(1-x)}]\frac{V}{GA}$$

We can define a penetration length l_p for the distance over which the constraint of the warping is important by setting $\omega l_p = 1$, which gives $l_p \approx h/3.5$. Clearly this means that the constraint of the warping is of no significance in normal beams. The effective E in isolators is of the order of several hundred times G, and the constraint of the warping at the ends will be effective over much larger distances from the ends in such cases.

3.2. Extension of Theory to Isolator

It is clear from the analysis of the warping of the short beam that selecting a warping function, f_w, that permits the uncoupling of the constitutive equations for bending moment M and warping resultant Q, is extremely convenient. For an isolator when the stress in the axial direction, we obtain the same result from

$$\nabla^2 p = \frac{12G}{t^3}w \tag{64}$$

which is the extension of the basic pressure solution for the elastomeric pad to variable vertical displacement $w(x,y)$. Eq. (64) by replacing p by $-\sigma_{11}$ and w/t by ε_{11}, we need to select $f_w(x_2)$ such that

$$\int_A \sigma_{11} x_2 dA$$

is independent of $\phi(x_1)$ and

$$\int_A \sigma_{11} f_w(x_2) dA$$

is independent of $\psi(x_1)$ when σ_{11} is given by

$$\nabla^2\sigma_{11} = -\frac{12G}{t^2}\varepsilon_{11} \tag{65}$$

A suitable selection of $f_w(x_2)$ is

$$f_w(x_2) = \frac{x_2^3}{h^3} - \frac{3}{7}\frac{x_2}{h} \tag{66}$$

and with this we have

$$u_1 = u(x_1) - \psi(x_1)x_2 + \phi(x_1)\left(\frac{x_2^3}{h^3} - \frac{3}{7}\frac{x_2}{h}\right) \tag{67}$$

$$u_2 = v(x_1) \tag{68}$$

from which

$$\varepsilon_{11} = u' - \psi'(x_1)x_2 + \phi(x_2)\left(\frac{x_2^3}{h^3} - \frac{3}{7}\frac{x_2}{h}\right)$$

The equation for σ_{11} becomes:

$$\frac{d^2}{dx_2^2}\sigma_{11} = -\frac{12G}{t^2}\left[u' - \psi' x_2 + \phi'\left(\frac{x_2^3}{h^3} - \frac{3}{7}\frac{x_2}{h}\right)\right]$$

and with $\sigma_{11} = 0$ at $x_2 = \pm h$ this leads to:

$$\sigma_{11} = \frac{6G}{t^2}h^2\left(\frac{x_2^2}{h^2} - 1\right)u' + \frac{2G}{t^2}h^3\left(\frac{x_2^3}{h^3} - \frac{x_2}{h}\right)\psi' - \frac{12Gh^2}{20t^2}\left(\frac{x_2^5}{h^5} - \frac{10}{7}\frac{x_2^3}{h^2} - \frac{3}{7}\frac{x_2}{h}\right)\phi' \tag{69}$$

Using previous definitions of M and Q leads to:

$$N = \frac{4Gh^2}{t^2}hu' = EAu' \tag{70}$$

$$M = \frac{8Gh^2}{15t^2}h^3\psi' = EI\psi' \tag{71}$$

and

$$Q = \frac{2Gh^2}{1225t^2}h\phi' = EJ\phi' \tag{72}$$

The other resultants can be calculated from

$$\sigma_{12} = G(v' - \psi) + C\phi\frac{3}{h}\left(\frac{x_2^2}{h^2} - \frac{1}{7}\right)$$

obtaining as before

$$V = GA(\upsilon' - \psi) + GB\phi \tag{73}$$

$$R = GB(\upsilon' - \psi) + GC\phi \tag{74}$$

where now

$$A = 2h \tag{75}$$

$$B = \frac{24}{21} \tag{76}$$

$$C = \frac{552}{245h} \tag{77}$$

The structure of the theory for non-buckling problems is now exactly the same as before with the values of the nominal *EI* and *EJ* being given in terms of G and the shape factor of a single layer, hlt, which may be quite large.

For the pure shear of an isolator in the absence of vertical load, the characteristic length of penetration of the restraint produced by the boundary condition at the ends of the bearing, which for the plain beam was

$$l_p \approx \sqrt{\frac{E}{35g}}h$$

is now given by

$$(\lambda l_p)^2 = 1$$

where

$$(\lambda l_p)^2 = \frac{GAGC - (GB)^2}{EJGA}l_p^2$$

with

$$EJ = \frac{2gh^2}{1225t^2}h$$

Thus

$$(\lambda l_p)^2 = 980\frac{l_p^2}{h^2}\frac{t^2}{h^2}$$

giving

$$l_p \approx \frac{h}{30}\frac{h}{t} \approx \frac{S}{30}h$$

where S is the shape factor. In this case then the penetration length is of the same order as the width of the bearing.

4. INTERACTION OF FIBER TENSION AND FIBER FLEXURE

Several examples of fiber-reinforced bearings were manufactured and tested in pairs in shear. The tested bearings are 12 inches in diameter and 4 inches thick, reinforced by Kevlar fiber. The bearing pair was loaded in compression to a pressure of 1000 psi and tested in shear to strain levels of 50%, 100%, and 150% (based on the full 4-inch thickness). Each test constituted three fully reversed cycles at each extreme shear strain level. The results of the tests are shown in Figures 15, 16 and 17.

The shear test results indicate that the extreme flexibility of the fiber reinforcement in bending has a small effect on the shear stiffness of the bearing, resulting in a reduction of the stiffness from the comparable steel-reinforced bearing to about 80-85%. An unexpected factor, however, is the level of damping shown by the fiber-reinforced bearings. The compound used in these bearings is an early example of high-damping bearing with an equivalent viscous damping of around 8% at 100% shear strain. In

the tests the damping is around 19% at 50% shear, 15% at 100% shear, and 14% at 150% shear, implying that the composite bearings are producing an energy dissipation that significantly exceeds that of the rubber compound. A possible explanation for this effect follows.

Each individual fiber of a single plane of reinforcement is made up of an extremely large number of single fibers twisted into a thread. The modulus of elasticity of the fiber material is extremely high of the order of 120 GPa (18 msi), and the possibility of extending or compressing of fibers at the outer edges of a thread is extremely unlikely. The flexure of the thread must happen by an interfacial slip of one fiber over another. The tension on the thread, induced by the vertical load through the lateral bulging of the rubber, causes an interfacial shear stress between the fibers in a single thread, and this frictional stress must be overcome before the threads can bend to accommodate the warping of the cross section.

Visualizing that each thread has a frictional moment, M_f, which has to be overcome and which remains constant during the deformation. It can be further postulated that the frictional moment depends on the value of the tension force, T_f, in the fiber, i.e.,

$$M_f = M_f(T_f)$$

and the instantaneous work done per unit length of the thread per unit time is

$$\dot{w} = M_f(T_f)\dot{K}_f$$

where $\dot{K}_f$ is the rate of change of fiber curvature. The sign of the curvature and the moment must be the same

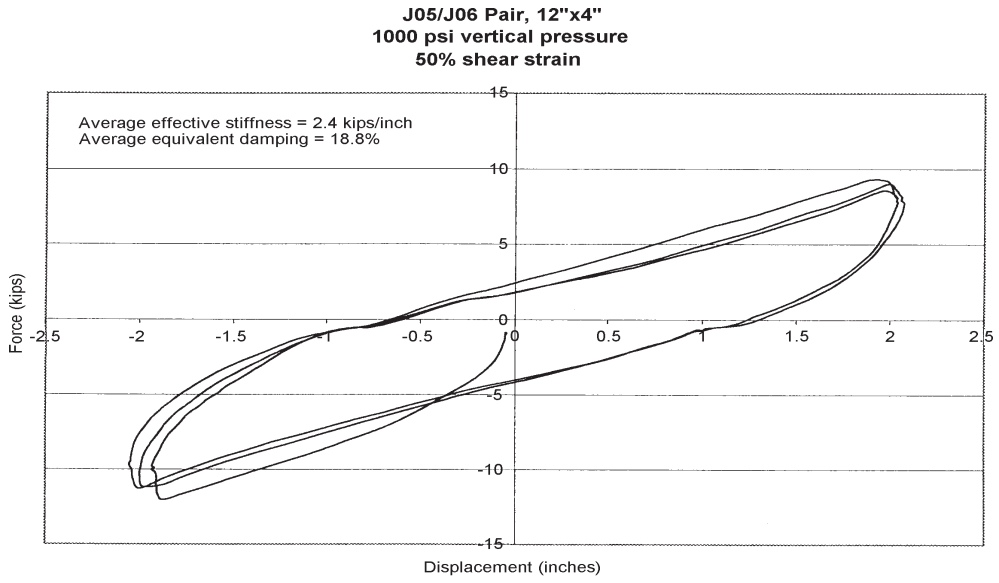

Figure 15. Compression-shear test of 12” diameter bearings to 50% shear strain.

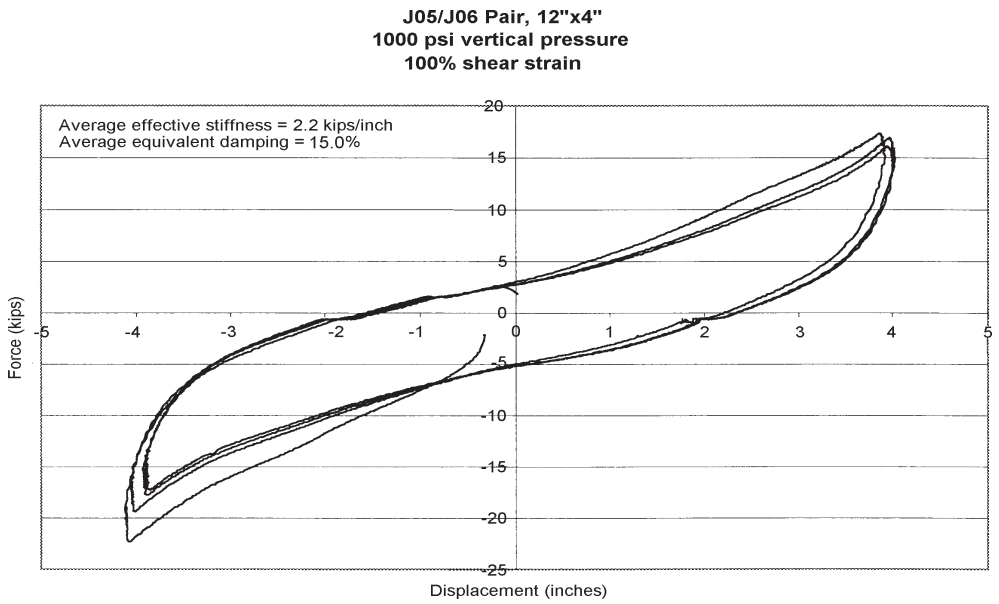

Figure 16. Compression-shear test of 12” diameter bearings to 100% shear strain.

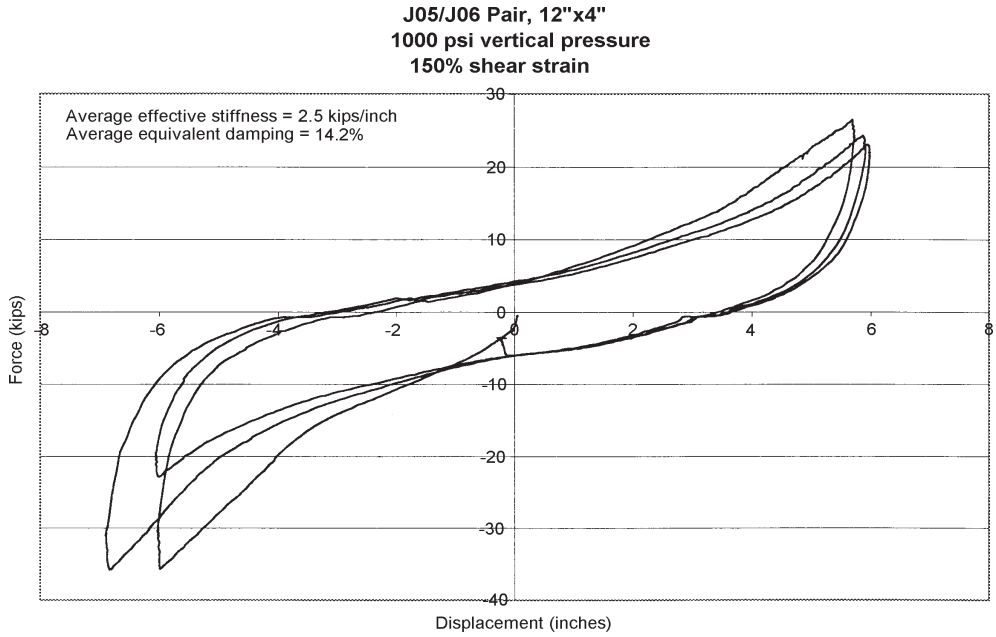

Figure 17. Compression-shear test of 12" diameter bearings to 150% shear strain (due to operator error, one cycle was to 175% shear strain).

to ensure that the rate of work is always positive.

The primary quantity of interest is the energy dissipated in the cycle (*EDC*) by the entire bearing; some of the *EDC* will come from the hysteresis of the elastomer and some from the fiber friction. If the bearing is subjected to a complete cycle of displacement with a maximum value D_{max}, then each element of thread will experience a maximum curvature K_{max}, which depends on the location of the reinforcing sheet in the bearing, denoted by the discrete variable x_i and position along the fiber denoted by the continuous variable y_f.

The total *EDC* then becomes:

$$EDC = \sum N_i \int_{\text{length of thread}} 4M_f(T_f)\, K_{max}(x_i, y_f)\, dy_f$$

$$T_f = T_f(x_i, y_f)$$

where N_i is the number of threads in a single sheet of reinforcement.

Of the various functions to appear in this equation all are known from the earlier analysis except the dependence of M_f on T_f. It is worth noting that T_f can be replaced in this by W since the analysis provides this dependence. Thus

$$EDC = 4W \sum_i N_i \phi_{max}(x_i) \int_{\text{length of thread}} f_r[(x_i), y_f]\, f_w''(x_i, y_f)\, dy_f$$

where K_{max} has been replaced by

$$K_{max} = \phi_{max} f_w''$$

and

$$T_f = W f_r$$

The minimal form for the dependence of M_f on T_f is

$$M_f = \alpha + \beta T_f$$

where α and β are constants to be determined from experimental work.

It is clear considerably more experimental work is needed to verify the hypothesis and to determine the various parameters that influence the energy dissipation. The concept is a very promising one, however, because currently it is difficult to incorporate high levels of intrinsic damping in natural rubber compounds by conventional means, such as adding carbon, oils, or resins, without degrading some of the advantageous properties of the elastomer. For isolators to be used for small buildings in highly seismic environments where the isolators are lightly loaded, it is advantageous to use an elastomer with a very low shear modulus (0.3-0.4 MPa), but such a compound will have low damping. If the fiber reinforcement can add significant damping, in the range of 10-15%, which is all that is needed in an isolation system [4], then even lower modulus elastomers could be used. The possibility then exists for continuous strip isolators is multi-story masonry wall buildings.

ACKNOWLEDGMENTS

The sample isolators were handmade by Ahmed Javid of Energy Research, Inc., San Jose, California. The bearing tests were carried out by Rodney Holland at the Mare Island Test Facility of Applied Structures Technology, LLC. The experimental part of the research was funded entirely by Energy Research, Inc.

REFERENCES

1. Rocard, Y. (1937). "Note sur le Calcul des Proprietes Elastique des Supports en Caoutchouc Adherent", *Journal de Physique et de Radium,* **8**, 197.

2. Gent, A.N., and Lindley, P.B. (1959). "Compression of Bonded Rubber Blocks", *Proceedings*, *Institution of Mechanical Engineers*, **173**(3), 111-122.

3. Gent, A.N., and Meinecke, E.A. (1970). "Compression, Bending and Shear of Bonded Rubber Blocks", *Ploymer Engineering and Science*, **10**(1), 48-53.

4. Kelly, J.M. (1999)."The Role of Damping in Seismic Isolation", *J. Earthquake Engineering and Structural Dynamics*, **28**(1), 3-20.